

A MODEL FOR TURBULENT PLANE COUETTE FLOW USING THE PROPER ORTHOGONAL DECOMPOSITION

Jeff Moehlis,^{1*} Troy Smith,² and Philip Holmes^{1,2}

¹ Program in Applied and Computational Mathematics, Princeton University, Princeton, NJ 08544, U.S.A.

² Department of Mechanical and Aerospace Engineering, Princeton University, Princeton, NJ 08544, U.S.A.

* Corresponding author: Jeff Moehlis, jmoehlis@math.princeton.edu

Abstract

We model turbulent plane Couette flow by expanding the velocity field as a sum of optimal modes calculated from a proper orthogonal decomposition of numerical data. Ordinary differential equations are obtained by performing a Galerkin projection of the Navier-Stokes equations onto these modes. For a truncation including only modes with no streamwise variation, we show under quite general conditions that the model has a linearly stable nontrivial fixed point; this corresponds physically to a state in which the mean flow is coupled to streamwise vortices and their associated streaks.

Introduction

Plane Couette flow (PCF) has many interesting properties, including (i) the linear stability of the laminar state for all Reynolds numbers Re [1], (ii) the experimental observation of turbulence for sufficiently high Re and/or perturbation amplitudes [2], and (iii) the existence of unstable finite amplitude solutions consisting of streamwise vortices and streaks which do not bifurcate from the laminar state [3, 4, 5]. Various ODE models have provided insight into these and other properties of PCF. For example, the models reviewed in [6] emphasize the non-normality of the linearized Navier-Stokes operator; this can give transient growth of perturbations even though the laminar state is linearly stable, and it is argued that if the growth is large enough then nonlinearities in the system may trigger a transition to turbulence. The model considered in [7, 8] views the turbulent state in terms of a nonlinear “self-sustaining process” involving streamwise rolls, streaks and their instabilities, and the mean flow. Stable fixed points or periodic orbits for the model are associated with the turbulent state. A related higher-dimensional model is considered in [9, 5], which suggest that the transition to turbulence is characterized by a chaotic repeller (cf. [10]).

In this paper, we present preliminary results from a different approach to modeling turbulent PCF. We start with data for the turbulent state obtained from numerical simulations. By performing a proper orthogonal decomposition (POD), we identify an energetically dominant set of empir-

ical eigenmodes (“POD modes”) from the data. We then construct a model by Galerkin projection of the Navier-Stokes equations onto this basis; this gives a set of coupled ODEs for the evolution of amplitudes of the POD modes. Because these modes optimally represent the energy of the system, it is hoped that low-dimensional models will capture important aspects of the turbulence. This method of deriving models has previously been applied, for example, to the turbulent boundary layer problem [11, 12]. Our model is also similar in some respects to those considered in [5, 7, 8, 9] except that instead of PCF, those consider sinusoidal shear flow which allows the use of simple trigonometric functions as a basis for the Galerkin expansion.

We begin by giving the governing equations for PCF. Next, we discuss the POD modes derived from turbulent PCF data. Finally, we describe preliminary results on a model obtained by projecting the governing equations onto the POD modes.

Governing Equations for PCF

In PCF, a fluid is sheared between two infinite parallel plates moving at speed U_0 , in opposite directions $\pm \mathbf{e}_x$. The x, y, z -directions are defined to be the streamwise, spanwise, and wall normal directions, respectively. We nondimensionalize lengths in units of $d/2$ where d is the gap between the plates, and velocities in units of U_0 . The laminar flow is then given by $\mathbf{U}_0 = z\mathbf{e}_x$, $z \in [-1, 1]$. The evolution equation for the per-

turbation $\mathbf{u}(\mathbf{x}, t)$ to the laminar flow is

$$\frac{\partial}{\partial t} \mathbf{u} = -(\mathbf{u} \cdot \nabla) \mathbf{u} - z \frac{\partial}{\partial x} \mathbf{u} - w \mathbf{e}_x - \nabla p + \frac{1}{Re} \nabla^2 \mathbf{u}, \quad (1)$$

where $Re \equiv U_0 d / (2\nu)$. The fluid is assumed to be incompressible, i.e., $\nabla \cdot \mathbf{u} = 0$, and there are no-slip boundary conditions at the plates. Finally, the flow is assumed to be periodic in the streamwise and spanwise directions, with lengths $L_x \equiv 4\pi$ and $L_y \equiv 2\pi$, respectively, following [5].

The POD modes for PCF

Details of the POD procedure are described in [12]; here we summarize key aspects. The POD modes $\Phi = (\Phi_1, \Phi_2, \Phi_3)$ are chosen to maximize the average projection of the perturbation $\mathbf{u} = (u_1, u_2, u_3)$ onto each mode. This leads to the eigenvalue problem

$$\sum_{j=1}^3 \int \int \int_{\Omega} \langle u_i(\mathbf{x}, t) u_j^*(\mathbf{x}', t) \rangle \Phi_{jn_x n_y}^{(n)}(\mathbf{x}') d^3 \mathbf{x}' \\ = \lambda_{n_x n_y}^{(n)} \Phi_{in_x n_y}^{(n)}(\mathbf{x}), \quad i = 1, 2, 3,$$

where $\langle \cdot \rangle$ is an (ensemble or time) averaging operation, $*$ denotes complex conjugation, and the “quantum numbers” $n \in \mathbb{Z}^+$, $n_x, n_y \in \mathbb{Z}$ distinguish different POD modes. The domain Ω is taken to be $0 \leq x \leq L_x$, $0 \leq y \leq L_y$, $-1 \leq z \leq 1$. The eigenvalue $\lambda_{n_x n_y}^{(n)}$ is twice the average kinetic energy in the POD mode $\Phi_{n_x n_y}^{(n)}$. The POD modes are orthogonal and will be normalized so that

$$\langle \Phi_{n_x n_y}^{(n)}, \Phi_{n'_x n'_y}^{(n')} \rangle = \delta_{nn'} \delta_{n_x n'_x} \delta_{n_y n'_y}.$$

Each POD mode will individually satisfy incompressibility and the appropriate boundary conditions. Also, the POD modes are optimal in the sense of capturing, on average, the most kinetic energy possible for a projection onto a given number of modes. We expand the perturbation velocity field \mathbf{u} in terms of POD modes as

$$\mathbf{u}(\mathbf{x}, t) = \sum_{n=1}^{\infty} \sum_{n_x=-\infty}^{\infty} \sum_{n_y=-\infty}^{\infty} a_{n_x n_y}^{(n)}(t) \Phi_{n_x n_y}^{(n)}(\mathbf{x}), \quad (2)$$

where the amplitudes $a_{n_x n_y}^{(n)}$ are complex unless $n_x = n_y = 0$, in which case they are real. The translation symmetry in the x and y -directions gives the (Fourier) decomposition [12]

$$\Phi_{n_x n_y}^{(n)}(\mathbf{x}) = \frac{\phi_{n_x n_y}^{(n)}(z)}{\sqrt{L_x L_y}} \exp\left(2\pi i \left(\frac{n_x x}{L_x} + \frac{n_y y}{L_y}\right)\right).$$

Table 1: Eigenvalues for the POD modes.

(n, n_x, n_y)	$\lambda_{n_x n_y}^{(n)}$	$\lambda_{n_x n_y}^{(n)} / \lambda_{00}^{(1)}$	$\% E_{n_x n_y}^{(n)}$
(1, 0, 0)	8.9246	1.0000	57.22
(1, 0, ± 2)	0.5804	0.0650	3.72
(1, 0, ± 1)	0.2807	0.0315	1.80
(1, ± 1 , ± 2)	0.0846	0.0095	0.54
(1, 0, ± 3)	0.0639	0.0072	0.41
(1, ± 1 , ± 1)	0.0522	0.0058	0.33
(2, 0, ± 2)	0.0499	0.0056	0.32
(2, 0, ± 1)	0.0489	0.0055	0.31
(1, ± 1 , ± 3)	0.0479	0.0054	0.31
...			

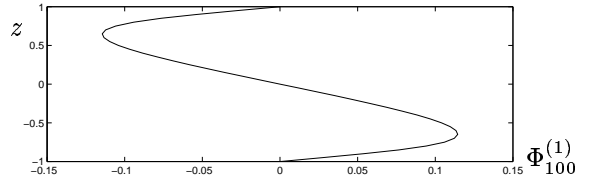


Figure 1: The x -component of the POD mode $\Phi_{00}^{(1)}$. The y and z -components are equal to zero.

Following the method of snapshots [13], $\langle \cdot \rangle$ is taken to be an average over snapshots from a single numerical run. In order to get a POD basis which retains the symmetries of the governing equations (in addition to translation symmetries, (1) is equivariant under spanwise reflections and rotation by π about the spanwise axis passing through the center of the domain), we also average over snapshots obtained by applying appropriate symmetry operations to the original snapshots (see e.g. [14]). Our results are obtained using data provided by Holger Faisst and Bruno Eckhardt from numerical simulations of fully developed turbulent flow in the plane Couette system at $Re = 400$. We use 1000 snapshots.

Table 1 shows the eigenvalues associated with the POD modes in decreasing order of magnitude. Here

$$\% E_{n_x n_y}^{(n)} = \left(\lambda_{n_x n_y}^{(n)} / \sum_{m, m_x, m_y} \lambda_{m_x m_y}^{(m)} \right) \times 100$$

is the percentage of average total energy contained in the (n, n_x, n_y) POD mode. Over half of the energy (57.22%) is contained in the (1, 0, 0) POD mode, which is shown in Figure 1. The next most energetic (1, 0, 1) and (1, 0, 2) POD modes, shown in Figure 2, consist of one and two pairs of streamwise rolls and associated streaks, respectively.

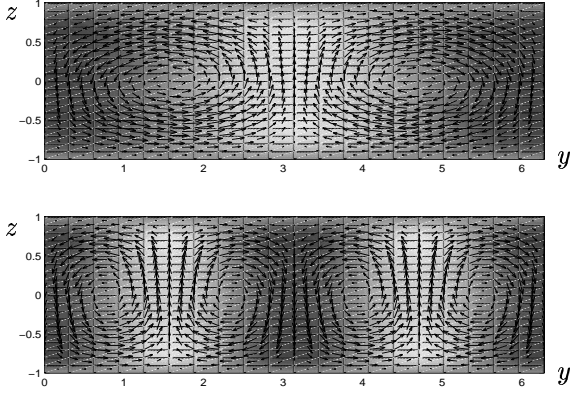


Figure 2: Flow fields \mathbf{u} associated with the (a) (1, 0, 1) and (b) (1, 0, 2) POD modes. The vectors show the spanwise and wall normal components of the velocity, while the dark (light) shading denotes positive (negative) streamwise velocity.

A Model for Turbulent PCF

Inserting (2) into (1) and performing a Galerkin projection, we obtain ODEs of the form

$$\dot{a}_{k_x k_y}^{(k)} = \sum_n \hat{A}_{k_x k_y}^{(k,n)} a_{k_x k_y}^{(n)} + [N(\mathbf{a}, \mathbf{a})]_{k k_x k_y}, \quad (3)$$

$$k = 1, 2, \dots, \quad k_x, k_y = \dots, -2, -1, 0, 1, 2, \dots,$$

where

$$[N(\mathbf{a}, \mathbf{a})]_{k k_x k_y} = \sum_{\substack{m, n \\ m_x, m_y}} \hat{B}_{k_x k_y m_x m_y}^{(k,m,n)} a_{m_x m_y}^{(m)} a_{k_x - m_x, k_y - m_y}^{(n)}.$$

The \hat{A} 's and \hat{B} 's are calculated from integrals of products of components of POD modes and their derivatives. Restrictions on the \hat{A} 's and \hat{B} 's follow from symmetry considerations. There are also conditions on the \hat{B} 's arising from the fact that nonlinear interactions redistribute energy without changing its total value. Finite dimensional models for turbulent PCF are obtained by truncating (3); here we consider truncations with $k = 1$, $k_x = 0$, and $-N_y \leq k_y \leq N_y$. Letting $a_{0j}^{(1)} \equiv r_j e^{i\theta_j}$ for $j = 0, \dots, N_y$ where $r_0 \in \mathcal{R}$, $r_j \geq 0$ for $j = 1, \dots, N_y$, we obtain

$$\dot{r}_0 = -A_0 r_0 + 2 \sum_{q=1}^{N_y} B_q r_q^2, \quad (4)$$

$$\dot{r}_j = (A_j - B_j r_0) r_j, \quad j = 1, \dots, N_y, \quad (5)$$

$$\dot{\theta}_0 \equiv 0, \quad \dot{\theta}_j = 0, \quad j = 1, \dots, N_y. \quad (6)$$

Here A_0 , the A_j 's, and the B_q 's are real, and numerically A_0 and the B_q 's are found to be positive. The coefficients A_j for $j = 0, \dots, N_y$ depend on Re , and may be positive or negative for

$j = 1, \dots, N_y$. However, at fixed Re we only need to consider modes with $A_j > 0$. This is because (4) and the positivity of the B_q 's imply that $r_0 < 0$ gives $\dot{r}_0 > 0$. Thus, eventually the system evolves to a state with $r_0 > 0$. From (5), modes with $A_j < 0$ therefore eventually decay to zero.

Equations (4,5) have a fixed point P_0 defined by $r_0 = r_1 = \dots = r_{N_y} = 0$, corresponding physically to the laminar state. Its eigenvalues $-A_0, A_1, \dots, A_{N_y}$ show that it is linearly unstable if any A_j is positive for $j \geq 1$. Equations (4,5) also have nontrivial fixed points P_l defined by $r_l = \bar{r}_l$, $r_0 = A_l/B_l$, and $r_j = 0$ for $j \neq 0, l$, where $\bar{r}_l \equiv (A_0 A_l / (2B_l^2))^{1/2}$ and $l = 1, \dots, N_y$. (Note from (6) that each P_l corresponds to a circle of fixed points in terms of the original amplitudes $a_{0j}^{(1)}$.) The eigenvalues of these fixed points are

$$\mu_{\pm}^{(l)} \equiv (-A_0 \pm (A_0^2 - 8A_0 A_l)^{1/2})/2$$

corresponding to perturbations in the (r_0, r_l) plane, and

$$\mu_q^{(l)} \equiv A_q - B_q A_l / B_l, \quad q \neq 0, l$$

corresponding to perturbations in the r_q -direction. The P_l fixed points correspond physically to states in which the mean flow is coupled to streamwise vortices and their associated streaks. Such states resemble the states associated with stable fixed points for the model considered in [7, 8].

Theorem The system (4,5) with $A_0 > 0$ and $A_j > 0, B_j > 0$ for $j = 1, \dots, N_y$ generically has (at least) one linearly stable nontrivial fixed point.

Proof The proof is by induction. Suppose $N_y = 1$. The fixed point P_1 has eigenvalues $\mu_{\pm}^{(1)}$ which must both have negative real part. Now suppose for the truncation at N_y that there is a linearly stable nontrivial fixed point, say P_L . The eigenvalues of P_L are $\mu_{\pm}^{(L)}$, both with negative real part, and

$$\mu_q^{(L)} < 0, \quad q = 1, 2, \dots, L-1, L+1, \dots, N_y. \quad (7)$$

For the truncation at $N_y + 1$, P_L has an additional eigenvalue $\mu_{N_y+1}^{(L)}$. If this is negative then P_L is linearly stable and the theorem is proved, so suppose instead that $\mu_{N_y+1}^{(L)} > 0$. The fixed point P_{N_y+1} has eigenvalues $\mu_{\pm}^{(N_y+1)}$, both with negative real part, and $\mu_q^{(N_y+1)}$, $q = 1, \dots, N_y$. By explicit computation

$$\mu_L^{(N_y+1)} = -\frac{B_L}{B_{N_y+1}} \mu_{N_y+1}^{(L)} < 0.$$

Finally, $\mu_{N_y+1}^{(L)} > 0$ implies that $A_{N_y+1}/B_{N_y+1} > A_L/B_L$, so

$$A_q - B_q A_{N_y+1}/B_{N_y+1} < A_q - B_q A_L/B_L = \mu_q^{(L)};$$

Table 2: Coefficients for equations (4,5) for $N_y = 6$.

j	A_j	B_j
0	$11.4349/Re$	–
1	$0.0688 - 5.5563/Re$	0.0117
2	$0.1738 - 10.8038/Re$	0.0264
3	$0.2218 - 15.3067/Re$	0.0325
4	$0.2414 - 22.0804/Re$	0.0336
5	$0.2324 - 30.2181/Re$	0.0339
6	$0.1968 - 41.0443/Re$	0.0289

Table 3: Fixed point properties for $N_y = 6$.

Fixed Pt	Existence	Stable Range
P_0	all Re	$Re < 62.16$
P_1	$Re > 80.76$	–
P_2	$Re > 62.16$	$62.16 < Re < 255.89$
P_3	$Re > 69.01$	$255.89 < Re < 517.30$
P_4	$Re > 91.47$	$Re > 517.30$
P_5	$Re > 130.03$	–
P_6	$Re > 208.56$	–

using (7), we conclude that

$$\mu_q^{(N_y+1)} < 0, \quad q = 1, 2, \dots, L-1, L+1, \dots, N_y.$$

Thus, P_{N_y+1} is linearly stable, and the theorem is proved.

As an example, we consider equations (4,5) with $N_y = 6$; this captures 69.87% of the average total energy. The coefficients and fixed point properties are given in Tables 2 and 3, respectively. We note that this model incorrectly predicts that the laminar state P_0 becomes linearly unstable for sufficiently high Re . As discussed in [15, 7], models derived using the expansion (2) and obtained from sustained turbulent data necessarily couple streamwise and cross-stream disturbances, which leads to instability of the laminar state. It is argued in [15] that models using an expansion which “properly” uncouples streamwise and cross-stream disturbances will correctly give stability for the laminar state; furthermore, the results found for models derived using expansion (2) will be strongly echoed in the results for models derived using the uncoupled expansion. We therefore view our “coupled” model as a model for sustained turbulence near $Re = 400$ and not for the transition to turbulence from the laminar state.

Conclusion

We have modeled turbulent plane Couette flow by expanding the velocity field in terms of POD modes calculated from numerical data.

ODEs were obtained by Galerkin projection of the Navier-Stokes equations onto these modes. For a truncation involving only modes with no streamwise variation, the model has a linearly stable non-trivial fixed point corresponding physically to a state in which the mean flow is coupled to streamwise vortices and their associated streaks. We continue to study this model and are currently extending it to include modes with streamwise variation which may lead to more complicated (and more realistic) dynamics.

Acknowledgements

We would like to thank Holger Faisst and Bruno Eckhardt for providing the data used for our POD analysis and also for helpful discussions. J.M. was supported by a National Science Foundation Mathematical Sciences Postdoctoral Research Fellowship, and T.S. and P.H. by DOE Grant FG02-95ER25238.

References

- [1] Drazin, P. and Reid, W.H., 1981, *Hydrodynamic Stability*, Cambridge University Press, Cambridge.
- [2] Dauchot, O. and Daviaud, F., 1995, *Phys. Fluids*, 7:335–343.
- [3] Nagata, M., 1990, *J. Fluid Mech.*, 217:519–527
- [4] Clever, R.M. and Busse, F.H., 1992, *J. Fluid Mech.*, 234:511–527.
- [5] Schmiegel, A., 1999, “Transition to turbulence in linearly stable shear flows”, Dissertation, University of Marburg.
- [6] Baggett, J.S. and Trefethen, L.N., 1997, *Phys. Fluids*, 9:1043–1053.
- [7] Waleffe, F., 1997, *Phys. Fluids*, 9:883–900.
- [8] Dauchot, O. and Vioujard, N., 2000, *Eur. Phys. J. B*, 14:377–381.
- [9] Eckhardt, B. and Mersmann, A., 1999, *Phys. Rev. E*, 60:509–517.
- [10] Schmiegel, A. and Eckhardt, B., 1997, *Phys. Rev. Lett.*, 79:5250–5253.
- [11] Aubry, N., Holmes, P., Lumley, J.L., and Stone, E., 1988, *J. Fluid Mech.*, 192:115–173.
- [12] Holmes, P., Lumley, J.L., and Berkooz, G., 1996, *Turbulence, Coherent Structures, Dynamical Systems and Symmetry*, Cambridge University Press, Cambridge.
- [13] Sirovich, L., 1987, *Quart. Appl. Math.*, XLV:561–590.
- [14] Smaoui, N. and Armbruster, D., 1997, *SIAM J. Sci. Comput.*, 18:1526–1532.
- [15] Berkooz, G., Holmes, P., and Lumley, J.L., 1991, *J. Fluid Mech.*, 230:75–95.